

Tennessee State University

Digital Scholarship @ Tennessee State University

Information Systems and Engineering
Management Research Publications

Center of Excellence in Information Systems
and Engineering Management

10-14-2010

New Precision Orbits of Bright Double-Lined Spectroscopic Binaries. V. The Am Stars HD 434 and 41 Sextantis

Francis C. Fekel
Tennessee State University

Michael H. Williamson
Tennessee State University

Follow this and additional works at: <https://digitalscholarship.tnstate.edu/coe-research>



Part of the [Stars, Interstellar Medium and the Galaxy Commons](#)

Recommended Citation

Francis C. Fekel and Michael H. Williamson 2010 AJ 140 1381

This Article is brought to you for free and open access by the Center of Excellence in Information Systems and Engineering Management at Digital Scholarship @ Tennessee State University. It has been accepted for inclusion in Information Systems and Engineering Management Research Publications by an authorized administrator of Digital Scholarship @ Tennessee State University. For more information, please contact XGE@Tnstate.edu.

NEW PRECISION ORBITS OF BRIGHT DOUBLE-LINED SPECTROSCOPIC BINARIES. V. THE AM STARS HD 434 AND 41 SEXTANTIS

FRANCIS C. FEKEL¹ AND MICHAEL H. WILLIAMSON

Center of Excellence in Information Systems, Tennessee State University, 3500 John A. Merritt Boulevard, Box 9501, Nashville, TN 37209, USA;
fekel@evans.tsuniv.edu

Received 2010 August 6; accepted 2010 August 27; published 2010 October 14

ABSTRACT

We have detected the secondary component in two previously known spectroscopic binaries, HD 434 and 41 Sex, and for the first time determined double-lined orbits for them. Despite the relatively long period of 34.26 days and a moderate eccentricity of 0.32, combined with the components' rotationally broadened lines, measurement of the primary and secondary radial velocities of HD 434 has enabled us to obtain significantly improved orbital elements. While the 41 Sex system has a much shorter period of 6.167 days and a circular orbit, the estimated V mag difference of 3.2 between its components also makes this a challenging system. The new orbital dimensions ($a_1 \sin i$ and $a_2 \sin i$) and minimum masses ($m_1 \sin^3 i$ and $m_2 \sin^3 i$) of HD 434 have accuracies of 0.8% or better, while the same quantities for 41 Sex are good to 0.5% or better. Both components of HD 434 are Am stars while the Am star primary of 41 Sex has a late-F or early-G companion. All four stars are on the main sequence. The two components of HD 434 are rotating much faster than their predicted pseudosynchronous velocities, while both components of 41 Sex are synchronously rotating. For the primary of 41 Sex, the spectrum line depth changes noted by Sreedhar Rao et al. were not detected.

Key words: binaries: spectroscopic – stars: individual (HD 434, 41 Sex)

1. INTRODUCTION

Direct determination of stellar masses and precise stellar parallaxes can be obtained from the three-dimensional orbits of binary stars that are resolved as both a spectroscopic and a visual binary. During the past two decades, major improvements in ground-based optical and near-infrared interferometry have produced a greater overlap of spectroscopic and visual binary domains (Quirrenbach 2001). Cunha et al. (2007) provided a list of over 30 interferometric visual orbits for double-lined spectroscopic binaries, while Torres et al. (2010) identified 23 interferometric systems with stellar masses determined to better than 3%. Work on individual systems (e.g., Hummel et al. 2001; Boden et al. 2006; Fekel et al. 2009a) has led to useful comparisons with evolutionary theory.

In SB9, the continually updated Web-based edition of the spectroscopic binary orbit catalog (Pourbaix et al. 2004), many of the older spectroscopic orbits have been computed with radial velocities from photographic plates. Because the photographic plates generally have lower resolutions and lower signal-to-noise ratios than modern CCD observations, results from them limit the precision of three-dimensional orbits. Thus, in previous papers of this series (Tomkin & Fekel 2006, 2008; Fekel et al. 2009b, 2010) we have obtained new radial velocities and computed spectroscopic orbits for bright field spectroscopic binaries, which are the most accessible systems to interferometry. These improved spectroscopic orbits will greatly enhance prospective interferometric observations of these systems.

To obtain the component masses and parallax of a binary system, spectroscopic orbits of the two components are needed. Although HD 434 and 41 Sex have only single-lined orbits in the literature, at red wavelengths the secondary components of

both spectroscopic binaries are visible, turning the two systems into viable candidates for three-dimensional orbital solutions.

The spectroscopic binaries, HD 434 and 41 Sex, that are analyzed in this paper have Am star primaries. Sreedhar Rao & Abhyankar (1992) previously examined the two systems together, revising their orbits and discussing the stars. Table 1 gives some of their basic properties.

2. BRIEF HISTORY

2.1. HD 434 = HIP 728 = SAO 73772

HD 434 ($\alpha = 00^{\text{h}}09^{\text{m}}00^{\text{s}}.16$, $\delta = 28^{\circ}14'51''.2$ (2000)) was not included in the Bright Star Catalogue (Hoffleit 1982), which has a nominal magnitude limit of $V = 6.5$. However, in Appendix III of that catalog it is noted as one of a number of stars that modern photoelectric photometry has shown to be slightly brighter than the catalog limiting magnitude (Hoffleit 1982). Interest in HD 434 came slowly. Shajn (1951) discovered that it had radial velocity variations and classified its spectrum as A2s. However, Walker (1966) identified it as an Am star. Palmer et al. (1968) observed HD 434 as part of a spectroscopic survey of 633 bright, northern A stars and confirmed its velocity variations. Eventually, Hube & Gulliver (1985) obtained over three dozen additional radial velocities from which they computed a preliminary single-lined orbit with a period of 34.2601 days. Both Sreedhar Rao & Abhyankar (1992) and Margoni et al. (1992) collected additional observations, and using previous velocity observations, the two groups independently revised the preliminary orbit of Hube & Gulliver (1985). As part of an extended project on Am binaries, Iliev et al. (2001) reobserved HD 434 and announced the discovery of its secondary spectrum. From those spectra, Budaj et al. (2003) obtained a mass ratio of 1.19 for the primary relative to the secondary.

Walker (1966) used the strength of the Ca K line relative to the Balmer lines to estimate a spectral class of A4, which was repeated by Palmer et al. (1968). Bertaud (1970) classified

¹ Visiting Astronomer, Kitt Peak National Observatory, National Optical Astronomy Observatory, operated by the Association of Universities for Research in Astronomy, Inc. under cooperative agreement with the National Science Foundation.

Table 1
Basic Properties of the Program Stars

Name	HR	HD	Spectral Type	V^a	$B - V^a$	Parallax ^b (mas)	Period (days)
...	...	434	Am	6.47	0.242	9.02	34.26
41 Sex	4237	93903	Am	5.80	0.156	10.50	6.17

Notes.

^a Perryman et al. (1997).

^b van Leeuwen (2007).

the Ca K and metal lines as A3 and F0, respectively. More recently Abt (2004) also identified the combined spectrum as that of a classical Am star and provided spectral classes for its Ca K, hydrogen, and metal lines of A2, A6, and F0, respectively. Examining their red wavelength spectra where both components of the binary were in evidence, Iliev et al. (2001) concluded that both stars have Am peculiarities.

Walker (1966) estimated a $v \sin i$ value of $60 \pm 25 \text{ km s}^{-1}$. However, the significantly higher resolution observations of Iliev et al. (2001) resulted in values of about 32 and 27 km s^{-1} for the primary and secondary, respectively.

2.2. 41 Sex = HR 4237 = HD 93903

Cowley et al. (1969) included 41 Sex ($\alpha = 10^{\text{h}}50^{\text{m}}18^{\text{s}}.06$, $\delta = -08^{\circ}53'51''.9$ (2000)) in a study of the spectral classifications of bright A stars. They characterized its spectrum as that of an Am star and found its Ca K line to have an A3 spectral class. Because most Am stars are binaries (Abt 1961; Abt & Levy 1985), Worek et al. (1978) obtained radial velocities of the system and, as expected, found it to be a spectroscopic binary. They determined an orbital period of 6.1670 days and concluded that it had a nearly circular orbit. Abt & Levy (1985) made 41 Sex part of their improved study of Am stars. From their spectroscopic observations they computed a new orbit that confirmed the results of Worek et al. (1978). Shortly thereafter, Worek et al. (1986) also published an improved solution of 41 Sex, which generally agreed with the previous two. Over the next dozen years, there were two additional attempts to upgrade the orbital solution of 41 Sex. Sreedhar Rao & Abhyankar (1992) combined all previously published velocities with an extensive number of newly obtained measurements to produce another revised orbit. Meanwhile, Worek (1998) continued his work on 41 Sex, computing the most recent revision of its orbit.

After the initial recognition of 41 Sex as an Am star by Cowley et al. (1969), Abt & Levy (1985) in their improved study of Am binaries classified the star as A2, A8, and F0 from its Ca K, hydrogen, and metal lines, respectively. Later, Abt & Morrell (1995) included 41 Sex in an extensive survey of A stars that examined the relationship between rotational velocity and spectral peculiarities. From their new analysis they estimated spectral classes of A3, A7, and A9, very similar to the results of Abt & Levy (1985). They also measured a $v \sin i$ value of 18 km s^{-1} for the primary. Royer et al. (2002) rescaled that result to 26 km s^{-1} , while Fekel (2003) obtained a value of 21 km s^{-1} .

From moderate dispersion photographic plates, Sreedhar Rao et al. (1990) announced the discovery of phase-modulated variations of the Ca K, hydrogen lines, and various metal lines in the spectrum of 41 Sex. They interpreted their results as surface abundance inhomogeneities similar to the Sr, Cr, and Eu line enhancements found in Ap stars and suggested that the characteristics of the abundance peculiarities linked the

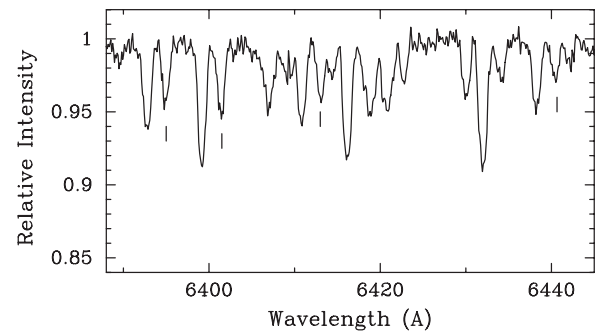


Figure 1. Spectrum of HD 434 in the 6430 Å region. Tick marks identify several redshifted secondary components.

heretofore separate Am and Ap stars. Although Sreedhar Rao & Abhyankar (1992) concluded that 41 Sex is a prototype for a new class of spectrum variables among Am stars, they did caution that higher resolution CCD spectra would be useful to confirm the spectral line variations. Worek (1998) took up their challenge and obtained CCD spectra of 41 Sex. His careful analysis of the new spectra did *not* confirm the line variability claims of Sreedhar Rao et al. (1990).

3. OBSERVATIONS AND RADIAL VELOCITIES

In 2005, a lone double-lined spectrum of HD 434 was acquired at McDonald Observatory with the 2.1 m telescope, the Sandiford Cassegrain echelle spectrograph (McCarthy et al. 1993), and a Reticon CCD. The spectrogram covers the wavelength range 5700–7000 Å and has a resolving power of 49,000.

From 2001 through 2010 we obtained spectrograms of both HD 434 and 41 Sex at the Kitt Peak National Observatory (KPNO) with the coudé feed telescope and coudé spectrograph. All observations were made with a TI CCD detector, and the spectra are centered at 6430 Å, cover a wavelength range of 84 Å, and have a resolution of 0.21 Å or a resolving power of just over 30,000. Further details about our observations and data reduction are given in Tomkin & Fekel (2006).

Finally, from 2003 through 2010 we collected an extensive number of observations of the two systems with the Tennessee State University 2 m Automatic Spectroscopic Telescope (AST), a fiber-fed echelle spectrograph, and a 2048×4096 SITE ST-002A CCD. The echelle spectrograms have 21 orders that cover the wavelength range 4920–7100 Å with an average resolution of 0.17 Å. The typical signal-to-noise ratio of these observations is ~ 80 . Eaton & Williamson (2004, 2007) have given a more extensive description of the telescope and spectrograph, operated at Fairborn Observatory near Washington Camp in the Patagonia Mountains of southeastern Arizona.

The spectra of the two systems show both components. However, for HD 434 the broad lines and low velocity amplitudes of the stars result in the lines of the two components being blended throughout much of the orbit. Fortunately, the components are completely separated at phases near periastron, as seen in Figure 1. For 41 Sex, the secondary lines are completely separated from their primary counterparts (Figure 2) at nearly all phases.

The procedures used to measure the McDonald and KPNO radial velocities have been described extensively in Tomkin & Fekel (2006). Here, we note that the McDonald velocities are absolute velocities, which were placed on a secure rest scale by means of the telluric O₂ and H₂O lines in the stellar spectra. The KPNO velocities were determined by cross-correlation with

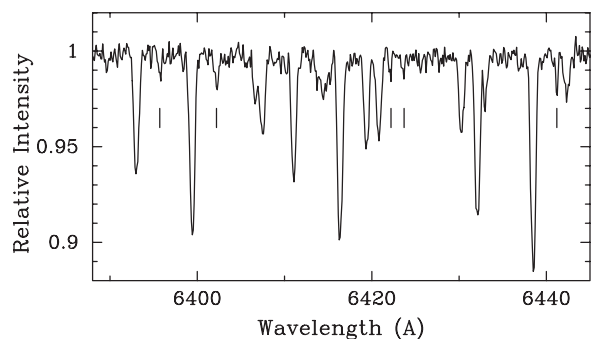


Figure 2. Spectrum of 41 Sex in the 6430 Å region. Tick marks identify several redshifted secondary components.

respect to IAU radial velocity standard stars of the same or similar spectral type as the program stars. The velocities adopted for those standards are from Scarfe et al. (1990).

Fekel et al. (2009b) provided an extensive general description of velocity measurement of the Fairborn AST spectra. Here, we mention that for HD 434 and 41 Sex the lines that were chosen for measurement were determined by the spectral classes of the stars. The component lines of the Am star HD 434 are roughly similar in strength, and the mean spectral class of the metal lines is F0 (Abt 2004). Thus, we used a line list that consists mostly of singly ionized elements such as Fe II, Si II, Ti II, and Cr II, which are prominent features in A and early-F stars. The primary of 41 Sex is also an Am star that has metal lines with a spectral class of about F0 (Abt & Levy 1985). However, to enhance our detection of the lines of the much cooler secondary, for both components we used a line list that consists mostly of Fe I lines, which is used for stars with spectral types of early-F through M, rather than the line list for A stars. The resulting Fairborn velocities, like those from McDonald Observatory, are absolute velocities. Our unpublished velocities of several IAU standard solar-type stars indicate that the Fairborn Observatory velocities have a small zero-point offset of -0.3 km s^{-1} relative to the velocities of Scarfe et al. (1990). Thus, we have added 0.3 km s^{-1} to each Fairborn velocity.

4. DETERMINATION OF ORBITS AND RESULTS

We have used several computer programs to determine the orbital elements. Preliminary orbits were computed with the program BISP (Wolfe et al. 1967), which implements a slightly modified version of the Wilsing-Russell method. Eccentric orbits were then determined with SB1 (Barker et al. 1967), a program that uses differential corrections. For a simultaneous solution of the two components of HD 434, we used SB2, which is a slightly modified version of SB1. For 41 Sex, circular orbits were determined with SB1C and SB2C (D. Barlow 1998, private communication), which also use differential corrections to compute improved orbital elements.

The spectra that we obtained at the different observatories have different wavelength ranges. Thus, different numbers of lines were available for measurement. In addition, the primary and secondary lines are of different quality because the components differ in strength and in line width. Thus, the velocity precision of each set of data will vary from observatory to observatory, and the precision will also usually differ for each primary and secondary component. To determine the weight for each set of our velocities, as well as those from the literature, we computed the variances of the individual orbital solutions, which are inversely proportional to our adopted weights.

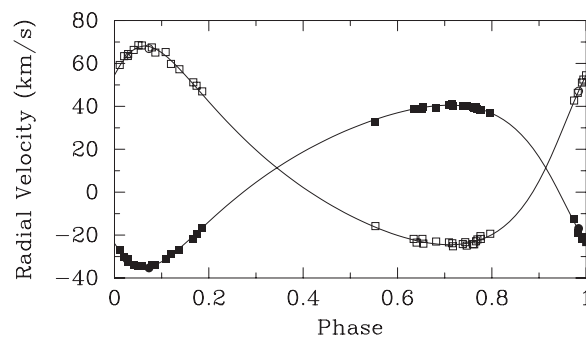


Figure 3. Radial velocities of HD 434 compared with the computed velocity curves. Filled and open symbols represent the primary and secondary, respectively. Squares, Fairborn Observatory; circles, KPNO; triangles, McDonald Observatory. Zero phase is a time of periastron passage.

4.1. HD 434

For HD 434 the line broadening and modest velocity amplitudes of its components, combined with its roughly 1 month orbital period, caused us to obtain the vast majority of our observations at Fairborn Observatory, where from 2003 through 2010 we acquired 39 spectra that had resolved or mostly resolved spectral lines of the two components. At McDonald Observatory and KPNO we collected only three additional double-lined spectra, one from McDonald and two from KPNO. All our velocities are listed in Table 2. Using the Fairborn velocities for the two components, we computed single-lined orbital solutions, which resulted in weights of 1.0 and 0.5 for the Fairborn primary and secondary velocities, respectively. Because of their small number, we simply adopted the same weights for the primary and secondary velocities of our three McDonald and KPNO observations. A simultaneous solution of the weighted primary and secondary velocities produced a period of 34.2624 days.

The spectral resolution of the various earlier photographic plate data sets was not sufficient to separate the components. Thus, the earlier velocity measurements are blends of the primary and secondary, and so we have not attempted to use those velocities to improve the orbit. Table 3 lists the orbital elements from our simultaneous solution of the two components with only our data. Figure 3 compares our primary and secondary velocities with the calculated velocity curves. Zero phase is a time of periastron passage.

In addition to our new elements, Table 3 lists the preliminary elements of Hube & Gulliver (1985), and there are significant differences between the two solutions. Our center-of-mass velocity is more than 4 km s^{-1} greater than that of Hube & Gulliver (1985), which is probably mostly due to their measurement of blended lines. In addition, our eccentricity is 20% smaller than that of Hube & Gulliver (1985), while our semiamplitude of the primary is 6% larger.

4.2. 41 Sex

For 41 Sex we acquired 34 observations at KPNO and 49 at Fairborn Observatory between 2001 and 2010 (Table 4). After measuring the primary and secondary velocities we computed four independent single-lined orbital solutions for the four data sets. Comparing the variances of those solutions, the KPNO velocities are the most precise, and we adopted weights of 1.0, 0.3, 0.04, and 0.01 for the KPNO primary, Fairborn primary, KPNO secondary, and Fairborn secondary velocities, respectively. The center-of-mass velocities of the four data sets are in good agreement except for that of the KPNO secondary.

Table 2
Radial Velocities of HD 434

Heliocentric Julian Date (HJD -2,400,000)	Phase	V_1 (km s ⁻¹)	$(O - C)_1$ (km s ⁻¹)	Wt_1	V_2 (km s ⁻¹)	$(O - C)_2$ (km s ⁻¹)	Wt_2	Source ^a
52966.736	0.716	41.2	0.7	1.0	-23.8	0.7	0.5	Fair
52967.675	0.744	40.3	0.2	1.0	-23.3	0.7	0.5	Fair
53032.665	0.640	39.0	0.0	1.0	-23.5	-0.9	0.5	Fair
53276.818	0.766	39.6	0.4	1.0	-22.9	-0.1	0.5	Fair
53285.789	0.028	-32.7	-1.1	1.0	63.5	-0.5	0.5	Fair
53290.782	0.174	-19.7	-0.7	1.0	49.6	1.0	0.5	Fair
53303.772	0.553	32.8	-1.1	1.0	-15.8	0.5	0.5	Fair
53310.852	0.760	39.8	0.3	1.0	-24.2	-1.0	0.5	Fair
53318.878	0.994	-21.0	0.8	1.0	52.5	0.5	0.5	Fair
53340.810	0.634	38.9	0.2	1.0	-21.8	0.5	0.5	Fair
53352.730	0.982	-19.1	-2.0	1.0	46.3	0.0	0.5	Fair
53353.726	0.011	-27.1	0.3	1.0	59.3	0.4	0.5	Fair
53359.718	0.186	-16.5	0.1	1.0	47.0	1.4	0.5	Fair
53649.879	0.655	39.9	0.4	1.0	-24.0	-0.7	0.5	Fair
53662.667	0.028	-31.3	0.2	1.0	63.6	-0.4	0.5	McD
53687.836	0.763	39.4	0.0	1.0	-24.3	-1.2	0.5	Fair
54003.775	0.984	-16.9	0.9	1.0	47.1	0.0	0.5	KPNO
54006.834	0.073	-35.3	-0.6	1.0	66.9	-1.0	0.5	KPNO
54860.584	0.991	-22.0	-1.4	1.0	51.1	0.5	0.5	Fair
54861.589	0.020	-30.1	-0.2	1.0	63.4	1.5	0.5	Fair
54862.628	0.051	-34.4	0.1	1.0	68.5	0.9	0.5	Fair
54863.605	0.079	-33.7	0.7	1.0	67.5	-0.1	0.5	Fair
54864.610	0.109	-31.1	0.1	1.0	65.3	1.7	0.5	Fair
54865.606	0.138	-26.9	-0.7	1.0	57.3	-0.2	0.5	Fair
54866.613	0.167	-21.7	-1.3	1.0	51.2	0.8	0.5	Fair
55159.574	0.718	40.4	-0.1	1.0	-25.2	-0.7	0.5	Fair
55160.573	0.747	40.1	0.1	1.0	-24.9	-1.1	0.5	Fair
55161.572	0.776	38.3	-0.4	1.0	-20.5	1.7	0.5	Fair
55332.910	0.777	38.2	-0.4	1.0	-21.8	0.3	0.5	Fair
55341.958	0.041	-33.8	-0.3	1.0	66.3	-0.1	0.5	Fair
55362.927	0.653	38.8	-0.7	1.0	-21.8	1.4	0.5	Fair
55363.927	0.682	39.4	-0.9	1.0	-23.0	1.1	0.5	Fair
55364.860	0.709	40.5	0.0	1.0	-23.4	1.1	0.5	Fair
55365.860	0.738	40.4	0.2	1.0	-24.2	-0.1	0.5	Fair
55366.928	0.769	38.7	-0.3	1.0	-22.0	0.6	0.5	Fair
55367.860	0.797	36.7	-0.3	1.0	-19.4	0.8	0.5	Fair
55373.948	0.974	-12.6	1.3	1.0	42.7	0.4	0.5	Fair
55374.818	1.000	-23.3	0.5	1.0	54.5	0.0	0.5	Fair
55375.818	0.029	-31.2	0.5	1.0	64.4	0.2	0.5	Fair
55376.818	0.058	-34.5	0.3	1.0	68.4	0.3	0.5	Fair
55377.798	0.087	-33.7	0.2	1.0	65.1	-1.7	0.5	Fair
55378.929	0.120	-28.9	0.6	1.0	59.8	-1.6	0.5	Fair

Note. ^a Fair, Fairborn Observatory; KPNO, Kitt Peak National Observatory; McD, McDonald Observatory.

Table 3
Orbital Elements and Related Parameters of HD 434

Parameter	Hube & Gulliver (1985)	This Study
P (days)	34.26014	34.26241 ± 0.00061
T (HJD)	2443041.27 ± 0.42	2454175.643 ± 0.043
e	0.405 ± 0.033	0.3200 ± 0.0038
ω_1 (deg)	140.9 ± 6.7	135.01 ± 0.55
K_1 (km s ⁻¹)	35.5 ± 1.7	37.74 ± 0.12
K_2 (km s ⁻¹)	...	46.33 ± 0.17
γ (km s ⁻¹)	6.9 ± 0.7	11.351 ± 0.093
$m_1 \sin^3 i$ (M_\odot)	...	0.9907 ± 0.0084
$m_2 \sin^3 i$ (M_\odot)	...	0.8071 ± 0.0063
$a_1 \sin i$ (10 ⁶ km)	15.30 ± 0.76	16.846 ± 0.059
$a_2 \sin i$ (10 ⁶ km)	...	20.680 ± 0.080
rms residual (km s ⁻¹) (unit weight)	...	0.7

Table 4
Radial Velocities of 41 Sex

Heliocentric Julian Date (HJD - 2,400,000)	Phase	V_1 (km s ⁻¹)	$(O - C)_1$ (km s ⁻¹)	Wt_1	V_2 (km s ⁻¹)	$(O - C)_2$ (km s ⁻¹)	Wt_2	Source ^a
52013.736	0.068	37.0	0.2	1.0	-89.9	0.4	0.04	KPNO
52015.737	0.393	-42.1	0.1	1.0	68.8	1.8	0.04	KPNO
52326.858	0.842	19.9	0.1	1.0	-53.4	3.1	0.04	KPNO
52327.851	0.003	40.9	-0.1	1.0	-98.9	-0.2	0.04	KPNO
52330.892	0.496	-52.3	0.0	1.0	86.6	-0.7	0.04	KPNO
52392.658	0.512	-52.4	-0.2	1.0	86.2	-0.9	0.04	KPNO
52395.697	0.004	40.8	-0.2	1.0	-100.8	-2.1	0.04	KPNO
52706.836	0.456	-50.6	0.0	1.0	84.3	0.4	0.04	KPNO
52707.818	0.616	-40.3	0.3	1.0	66.2	2.3	0.04	KPNO
52755.730	0.385	-40.4	0.2	1.0	65.2	1.2	0.04	KPNO
52756.708	0.543	-50.4	0.2	1.0	85.8	1.9	0.04	KPNO
52758.723	0.870	26.2	-0.1	1.0	-68.2	1.2	0.04	KPNO
53022.954	0.716	-15.4	0.2	0.3	12.7	-1.4	0.01	Fair
53023.961	0.879	27.8	-0.4	0.3	-74.9	-1.7	0.01	Fair
53051.903	0.410	-45.7	-0.6	0.3	71.6	-1.3	0.01	Fair
53119.753	0.412	-45.5	-0.1	1.0	74.5	1.0	0.04	KPNO
53120.719	0.569	-47.8	0.3	1.0	78.0	-0.8	0.04	KPNO
53139.699	0.646	-34.0	0.0	0.3	51.7	1.0	0.01	Fair
53167.674	0.183	12.8	-0.7	0.3	-44.8	-0.9	0.01	Fair
53169.642	0.502	-52.3	0.1	1.0	89.0	1.6	0.04	KPNO
53172.641	0.988	40.8	-0.1	1.0	-98.4	0.1	0.04	KPNO
53288.020	0.697	-20.8	0.1	0.3	24.8	0.1	0.01	Fair
53313.953	0.902	32.3	-0.2	0.3	-84.3	-2.6	0.01	Fair
53323.000	0.369	-38.3	-0.8	0.3	56.1	-1.6	0.01	Fair
53333.894	0.136	24.8	-0.2	0.3	-66.2	0.7	0.01	Fair
53352.022	0.075	35.8	-0.1	0.3	-89.3	-0.8	0.01	Fair
53358.856	0.183	13.7	0.4	0.3	-45.7	-2.2	0.01	Fair
53367.998	0.666	-29.9	-0.7	0.3	42.2	0.9	0.01	Fair
53372.000	0.315	-23.5	0.6	0.3	31.7	0.6	0.01	Fair
53401.032	0.022	40.7	0.2	0.3	-96.0	1.8	0.01	Fair
53425.890	0.053	38.5	0.1	0.3	-91.5	2.1	0.01	Fair
53426.910	0.219	3.1	-0.4	0.3	-22.7	1.3	0.01	Fair
53439.848	0.316	-25.1	-0.5	0.3	32.6	0.5	0.01	Fair
53452.781	0.414	-45.9	-0.3	0.3	74.4	0.4	0.01	Fair
53465.745	0.516	-52.3	-0.2	0.3	89.7	2.8	0.01	Fair
53478.776	0.629	-38.2	-0.3	0.3	57.5	-1.1	0.01	Fair
53487.764	0.086	34.0	-0.3	1.0	-84.6	0.8	0.04	KPNO
53490.753	0.571	-48.0	-0.2	1.0	77.3	-1.0	0.04	KPNO
53492.728	0.891	30.2	-0.3	1.0	-74.7	3.1	0.04	KPNO
53504.681	0.829	17.0	0.4	0.3	-49.2	1.0	0.01	Fair
53527.681	0.559	-49.1	0.1	0.3	80.3	-0.8	0.01	Fair
53534.634	0.686	-23.5	0.4	1.0	31.1	0.5	0.04	KPNO
53535.633	0.848	21.5	0.2	1.0	-56.4	3.2	0.04	KPNO
53536.634	0.011	40.8	-0.1	1.0	-98.6	-0.1	0.04	KPNO
53724.031	0.398	-43.1	-0.1	0.3	66.5	-2.3	0.01	Fair
53737.010	0.502	-52.5	-0.1	0.3	85.3	-2.1	0.01	Fair
53763.933	0.868	25.6	-0.2	0.3	-64.8	3.6	0.01	Fair
53850.735	0.943	38.2	0.2	1.0	-91.7	1.1	0.04	KPNO
53851.728	0.104	31.4	0.0	1.0	-81.6	-2.0	0.04	KPNO
53856.706	0.911	33.6	-0.3	1.0	-84.8	-0.2	0.04	KPNO
54220.697	0.933	36.9	-0.1	1.0	-91.4	-0.7	0.04	KPNO
54264.652	0.061	38.0	0.4	1.0	-92.7	-0.7	0.04	KPNO
54526.782	0.566	-48.6	-0.2	1.0	78.3	-1.2	0.04	KPNO
54582.774	0.645	-33.9	0.3	1.0	52.9	1.6	0.04	KPNO
54849.905	0.961	39.4	-0.2	0.3	-92.0	4.0	0.01	Fair
54898.842	0.897	31.5	0.0	0.3	-80.7	-0.9	0.01	Fair
54905.905	0.042	39.2	-0.2	0.3	-95.6	-0.1	0.01	Fair
54918.850	0.141	23.0	-0.9	0.3	-66.2	-1.6	0.01	Fair
54946.713	0.659	-31.1	-0.2	1.0	46.0	1.3	0.04	KPNO
54948.713	0.983	41.0	0.3	0.3	-94.1	4.1	0.01	Fair
54982.735 ^b	0.500	-53.3	-0.9	0.3	Fair
55006.636	0.376	-38.6	0.2	1.0	62.5	2.1	0.04	KPNO
55159.008	0.083	34.4	-0.3	0.3	-86.7	-0.4	0.01	Fair
55234.899 ^b	0.389	-41.9	-0.4	0.3	Fair
55241.849	0.516	-52.3	-0.2	0.3	86.9	0.0	0.01	Fair

Table 4
(Continued)

Heliocentric Julian Date (HJD $-2,400,000$)	Phase	V_1 (km s^{-1})	$(O - C)_1$ (km s^{-1})	Wt_1	V_2 (km s^{-1})	$(O - C)_2$ (km s^{-1})	Wt_2	Source ^a
55247.962	0.507	-52.8	-0.5	0.3	84.3	-3.0	0.01	Fair
55269.838	0.055	38.2	-0.1	0.3	-92.9	0.4	0.01	Fair
55275.791	0.020	40.6	0.0	0.3	-96.0	2.0	0.01	Fair
55280.804	0.833	17.8	0.3	0.3	-53.1	-1.2	0.01	Fair
55286.751	0.797	8.3	0.4	0.3	-31.0	1.8	0.01	Fair
55291.757	0.609	-42.3	-0.4	0.3	64.3	-2.1	0.01	Fair
55300.711	0.061	37.5	-0.1	0.3	-92.5	-0.5	0.01	Fair
55307.718	0.197	9.4	-0.2	0.3	-36.5	-0.4	0.01	Fair
55311.752	0.851	21.7	-0.3	1.0	-59.0	1.9	0.04	KPNO
55312.771	0.016	41.1	0.4	1.0	-99.5	-1.2	0.04	KPNO
55314.753	0.338	-30.0	0.1	0.3	42.9	-0.1	0.01	Fair
55318.809	0.995	41.8	0.8	0.3	-98.9	-0.2	0.01	Fair
55324.667	0.945	38.9	0.6	0.3	-92.6	0.7	0.01	Fair
55328.698	0.599	-43.2	0.4	0.3	69.9	-0.1	0.01	Fair
55334.677	0.568	-47.8	0.3	0.3	78.9	0.0	0.01	Fair
55342.682	0.866	25.6	0.1	0.3	-68.1	-0.2	0.01	Fair
55347.681	0.677	-26.8	-0.5	0.3	33.6	-1.9	0.01	Fair
55365.645	0.590	-45.1	0.0	1.0	72.3	-0.6	0.04	KPNO
55368.634	0.075	35.7	-0.2	1.0	-90.1	-1.4	0.04	KPNO

Notes.

^a Fair, Fairborn Observatory; KPNO, Kitt Peak National Observatory.

^b Low S/N spectrum, secondary too weak to be measured.

However, given that its velocities typically come from the measurement of just one or two very weak secondary lines, the 1 km s^{-1} difference between the primary and secondary center-of-mass values is not overly troubling. A simultaneous solution of the appropriately weighted primary and secondary velocities produced a period of 6.167019 days.

From their initial orbital analysis, Worek et al. (1978) concluded that the orbit of 41 Sex is essentially circular. Follow-up work generally validated that result. However, Sreedhar Rao & Abhyankar (1992) concluded that the very modest eccentricity of 0.034, which they obtained for their combined solution, is real. Our independent KPNO and Fairborn orbital solutions of the primary produce extremely small eccentricities of 0.0016 ± 0.0017 and 0.0009 ± 0.016 , respectively. Thus, following the precepts of Lucy & Sweeney (1971) we have concluded that the orbit is indeed circular.

In principle, the older literature velocities of the primary could improve the precision of the period. However, the vast majority are from photographic plates that have significantly lower resolution than our observations. Nevertheless, we have examined two different older data sets. The 22 KPNO photographic plate velocities of Abt & Levy (1985) were obtained between 1976 and 1978, extending the time baseline by 25 years. However, from a comparison of orbital solutions the weights of those velocities, relative to our KPNO CCD velocities, are just 0.01. The resulting combined solution of the two data sets does not significantly change the orbital period. We also examined the six CCD velocities of Worek (1998) to see how they compare with our orbit for the primary. Although they appear to be consistent with our orbit, they have residuals that on average are 0.9 km s^{-1} too positive. This is not overly surprising because such a value is similar to the difference between our systemic velocity and his (-5.7 and -4.5 km s^{-1} , respectively). Therefore, we have chosen to list in Table 5 the circular orbital solution determined with the new velocities from our two observatories. Figure 4 compares our primary and secondary velocities with the calcu-

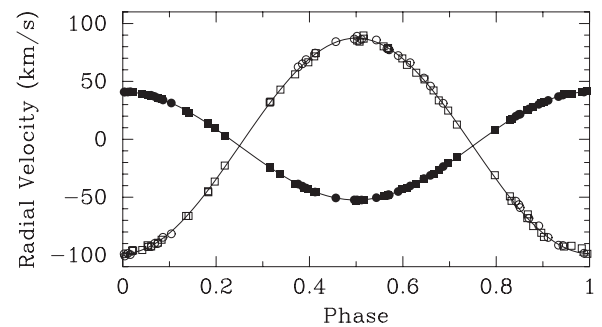


Figure 4. Radial velocities of 41 Sex compared with the computed velocity curves. Filled and open symbols represent the primary and secondary, respectively. Circles, KPNO; squares, Fairborn Observatory. Zero phase is a time of maximum velocity of the primary.

lated velocity curves. For a circular orbit, the element T , a time of periastron passage, is undefined. Thus, as recommended by Batten et al. (1989), T_0 , a time of maximum velocity for the primary, is used instead.

In addition to our elements, Table 5 lists those of Abt & Levy (1985) and Worek (1998). The derived periods and semiamplitudes of the three solutions are in excellent accord. The three values of the systemic velocity are -6.2 , -4.5 , and -5.7 km s^{-1} according to Abt & Levy (1985), Worek (1998), and this work. The uncertainties of the values indicate that the difference between the systemic velocity of Abt & Levy (1985) and our work is slightly more than 1σ . The 1.2 km s^{-1} difference between the results of Worek (1998) and our work is a 6σ result, but nevertheless, perhaps is simply a difference in observatory zero points rather than an indication of a third star in the system. We note that our velocities cover 10 years and are more precise than those previously obtained, yet they show no systematic, long-term velocity change attributable to a third star.

Table 5
Orbital Elements and Related Parameters of 41 Sex

Parameter	Abt & Levy (1985)	Worek (1998)	This Study
P (days)	6.16663 ± 0.00002	6.16699 ± 0.00002	6.1670194 ± 0.0000070
T_0 (HJD)	2440000.162 ± 0.012	2444730.060 ± 0.006	2453690.7442 ± 0.0011
e	0.025 ± 0.010	0.014 ± 0.006	0.0 (adopted)
ω_1 (deg)	0.0 ± 0.7	272 ± 24	...
K_1 (km s ⁻¹)	46.9 ± 0.5	46.8 ± 0.3	46.670 ± 0.040
K_2 (km s ⁻¹)	93.06 ± 0.20
γ (km s ⁻¹)	-6.2 ± 0.4	-4.5 ± 0.2	-5.685 ± 0.033
$m_1 \sin^3 i$ (M_\odot)	1.1637 ± 0.0060
$m_2 \sin^3 i$ (M_\odot)	0.5836 ± 0.0019
$a_1 \sin i$ (10^6 km)	3.976	3.97 ± 0.03	3.9577 ± 0.0034
$a_2 \sin i$ (10^6 km)	7.892 ± 0.017
rms residual (km s ⁻¹) (unit weight)	1.97	1.5	0.2

5. SPECTRAL TYPES AND MAGNITUDE DIFFERENCE

Strassmeier & Fekel (1990) identified several luminosity-sensitive and temperature-sensitive line ratios in the 6430–6465 Å region. They employed those critical line ratios and the general appearance of the spectrum as spectral-type criteria. As discussed below, the abundance peculiarities of the A stars that dominate our systems make normal spectral classification essentially impossible in our limited 84 Å region. In addition, for stars that are hotter than early-G spectral class, the line ratios in that wavelength region have little sensitivity to luminosity. However, the luminosity class may be determined by computing the absolute visual magnitude with the *Hipparcos* parallax and comparing that magnitude to evolutionary tracks or a table of canonical values for giants and dwarfs.

Spectra of our two binaries were compared with the spectra of a number of A, F, and early-G stars primarily from the lists of Abt & Morrell (1995) and Fekel (1997). The reference star spectra were obtained at KPNO with the same telescope, spectrograph, and detector as our binary star spectra. To facilitate a comparison, various combinations of the reference-star spectra were rotationally broadened, shifted in radial velocity, appropriately weighted, and added together with a computer program developed by Huenemoerder & Barden (1984) and Barden (1985) in an attempt to reproduce the binary spectra.

Analysis of our two star systems has met with very limited success because three of the four components are Am stars and lines of the fourth component are extremely weak. Classical Am stars have spectral classes of A4–F1, determined from their hydrogen lines (Abt & Morrell 1995). Such stars are noted as having peculiar spectra because lines of their metallic elements such as iron and strontium are stronger than expected compared to the hydrogen classification, while elements such as calcium and scandium are weaker (Abt & Morrell 1995). There are no hydrogen lines in our limited 6430 Å wavelength region, and the iron and calcium abundance peculiarities vary from star to star, making it impossible to adequately characterize the combined spectrum of the two components with our limited number of reference spectra.

5.1. HD 434

Despite being unable to determine spectral classes for the components of HD 434, we have compared the spectrum of this binary with several reference star spectra and have the following comments.

Abt (2004) classified the combined spectrum of HD 434 as an Am star with A2, A6, and F0 spectral classes for its

Ca K, hydrogen, and metal lines, respectively. We find that in the 6430 Å region, the spectrum of the Am star HR 7431, which Abt & Morrell (1995) classified as A2, A7, and F0, is a reasonable fit to the relative strength of the primary's iron and calcium lines. Thus, we adopt A2 and F0 for the calcium and metal spectral classes of the primary. The iron lines of the secondary are more consistent with those of HR 5075, classified as F2 V by Abt & Morrell (1995), than with those of HR 7431, but the calcium lines of the secondary are much weaker than those of HR 5075, and so we adopt A2 and F2 for the calcium and metal spectral classes of the secondary. Thus, we confirm the conclusion of Iliev et al. (2001) that both components are Am stars. From our various spectrum fits to the iron lines, we estimate a V mag difference of 0.8 ± 0.2 . This assumes that the surface abundances of the two stars are the same, which, because both components are Am stars, is not necessarily the case. However, a similar or identical magnitude difference can be estimated from the mass ratio of HD 434 and the canonical properties of A and early-F stars, if one assumes that the spectral type of the primary is somewhat earlier than the composite hydrogen type of Abt (2004) and that the secondary type is somewhat later. For example, in his Table B1, Gray (1992) lists masses for A5 V and F1 V stars of $1.86 M_\odot$ and $1.51 M_\odot$, respectively. This combination results in a mass ratio of 0.81, identical to our mass ratio for HD 434 from Table 3. Those two spectral types have corresponding M_v magnitudes of 2.0 and 2.8, resulting in a magnitude difference of 0.8, which is the value that we have estimated from our spectrum fits to the iron lines.

5.2. 41 Sex

Because the primary of 41 Sex, like both components of HD 434, is an Am star, we are unable to determine its hydrogen line spectral class. The large magnitude difference between the primary and the secondary means that the secondary spectral class is not well determined. Nevertheless, we discuss the results of our comparison of the spectrum of 41 Sex with several reference star spectra.

Abt & Morrell (1995) classified the combined spectrum of 41 Sex as an Am star with A3, A7, and A9 for its Ca K, hydrogen, and metal lines, respectively. We find that in the 6430 Å region, the spectrum of the Am star HR 7431, which Abt & Morrell (1995) classified as A2, A7, and F0 for its Ca K, hydrogen, and metal lines, respectively, is a reasonable fit to the relative strength of the primary's Fe I and Fe II lines but its calcium lines are not nearly as strong as those of 41 Sex. From a comparison with several other reference stars we adopt A5 and F0 for the primary's calcium and metal spectral classes, respectively. The

very weak spectrum of the secondary is consistent with that of a late-F or an early-G star.

6. BASIC PROPERTIES

6.1. HD 434

For HD 434 we begin by adopting a V mag of 6.47 and a $B - V$ color of 0.242 mag from the *Hipparcos* catalog (Perryman et al. 1997). With our magnitude difference of 0.8, the individual V magnitudes are 6.89 and 7.69 for the primary and secondary, respectively. The new *Hipparcos* parallax reduction by van Leeuwen (2007) produces a value of 9.02 ± 0.49 mas and corresponds to a distance of 110.9 ± 6.0 pc. Even though there may be a slight amount of reddening at this distance, we assume that it is negligible. The resulting absolute magnitudes are $M_V = 1.7 \pm 0.2$ mag and $M_V = 2.5 \pm 0.2$ mag for the primary and secondary, respectively. From Johnson (1966) we assume $B - V$ colors of 0.17 for the primary and 0.36 for the secondary, which, when combined for the two stars, produce a $B - V$ color similar to the observed value. Then, from Table 3 of Flower (1996), we obtain the bolometric corrections and effective temperatures of the two components. Finally, with the use of the Stefan–Boltzmann law, the luminosities of the primary and secondary are $L_1 = 16.7 \pm 3.6 L_\odot$ and $L_2 = 8.0 \pm 1.7 L_\odot$, respectively, while the radii are $R_1 = 2.2 \pm 0.3 R_\odot$ and $R_2 = 2.0 \pm 0.3 R_\odot$, respectively. The uncertainties in the computed quantities are dominated by the parallax uncertainty, the magnitude difference uncertainty, and the effective temperature uncertainty with the latter estimated to be ± 300 K.

6.2. 41 Sex

Stockton & Fekel (1992) concluded that binaries with mass ratios as small as 0.6 and magnitude differences somewhat greater than 2.5 mag can be detected at 6430 Å. With a smaller mass ratio of 0.5, the components of 41 Sex have an even greater magnitude difference. Because of the faintness of the secondary, that component will have only a very slight effect on the V mag and color of the primary. For example, if the ΔV mag between the primary and secondary is assumed to be 3.0 mag, then the V mag of the primary is 5.87, while increasing the magnitude difference to 3.5 makes the V mag of the primary 5.84. As discussed below, in the following computations we adopt $\Delta V = 3.2$ mag, which with a V mag of 5.80 for the combined system from *Hipparcos* (Perryman et al. 1997) results in $V = 5.86$ mag for the primary. The new reduction of the *Hipparcos* parallax produces a value of 10.50 ± 0.34 mas (van Leeuwen 2007), which corresponds to a distance of 95.2 ± 3.1 pc. At such a distance we assume that the system is not significantly reddened. Our assumed magnitude difference and the parallax result in an absolute magnitude of $M_V = 0.97 \pm 0.12$ mag for the primary. From the *Hipparcos* catalog (Perryman et al. 1997), the $B - V$ color of the 41 Sex system is 0.156. Given the very modest effect of the secondary, we adopt a slightly smaller value of 0.15 for the primary. The bolometric correction and effective temperature come from Table 3 of Flower (1996). Then from the Stefan–Boltzmann law the luminosity of the primary, L_1 , is $31.9 \pm 3.6 L_\odot$, while the radius is $R_1 = 2.9 \pm 0.2 R_\odot$.

The properties of the secondary are much less secure. We compare the M_V of the primary and the components' mass ratio with the canonical stellar properties listed in Table B1 of Gray (1992) and conclude that the secondary is most probably a late-F or early-G star, which is in agreement with our rough

classification of this star. From that table we estimate a V mag difference of 3.2 ± 0.3 . This leads to $L_2 = 1.8 \pm 0.5 L_\odot$ and $R_2 = 1.3 \pm 0.2 R_\odot$. The uncertainties in the computed quantities of the primary and secondary are dominated by the parallax and the effective temperature uncertainties as well as the magnitude difference for the secondary. The temperature uncertainty is estimated to be ± 200 K for the primary and secondary.

7. CIRCULARIZATION AND SYNCHRONIZATION

The two main theories of orbital circularization and rotational synchronization (see Zahn 1977; Tassoul & Tassoul 1992) disagree significantly on absolute time scales but do agree that synchronization should occur first. Observationally, Matthews & Mathieu (1992) examined 62 spectroscopic binaries with A-type primaries and periods less than 100 days. They concluded that all systems with orbital periods $\lesssim 3$ days have circular or nearly circular orbits. They also found that many binaries with periods in the range of 3–10 days have circular orbits. With a period of 34.26 days it is not surprising that HD 434 still has an eccentric orbit. Also unsurprising is the circular orbit of 41 Sex, which has a period of only 6.167 days.

In an eccentric orbit, Hut (1981) has shown that the rotational angular velocity of a star will tend to synchronize with that of the orbital motion at periastron. For HD 434 we compute the pseudosynchronous period with Equation (42) of Hut (1981).

To help in assessing pseudosynchronization and synchronization in our two binaries, we have determined projected rotational velocities from our red-wavelength KPNO spectra with the procedure of Fekel (1997). For A-type stars the measured line broadening was converted to a $v \sin i$ value. For stars with later spectral classes, macroturbulent broadening has been taken into account. Following Fekel (1997), for late-F and early-G stars a value of 3 km s^{-1} was used. To convert the $v \sin i$ values into equatorial rotational velocities, we assume, as is generally done, that the axes of the orbital and rotational planes are parallel, so the inclinations are equal.

7.1. HD 434

To determine whether the components of HD 434 are rotating pseudosynchronously, we compare our observed velocities with the predicted pseudosynchronous velocities. For HD 434 our $v \sin i$ values, averaged from two spectra, are 33 ± 2.0 and $30 \pm 3.0 \text{ km s}^{-1}$ for the primary and secondary, respectively. These values are in good agreement with those of Iliev et al. (2001), who estimated projected rotational velocities of about 32 and 27 km s^{-1} for the two stars. The minimum masses of the two components are relatively small; both are less than $1 M_\odot$. From our comparison with the solar-abundance evolutionary tracks of Girardi et al. (2000) we adopt a mass of $1.9 M_\odot$ for the primary (Figure 5). Then that mass, combined with its $m \sin^3 i$ value (Table 3), results in an orbital inclination of 54° . If the rotational inclination is the same as that of the orbit, then the observed equatorial rotational velocities are 40 and 33 km s^{-1} for the primary and secondary, respectively. The pseudosynchronous rotation period of HD 434 is 20.9 days. This value plus our computed radii from the Stefan–Boltzmann law produces pseudosynchronous rotational velocities of 5 km s^{-1} for both the primary and secondary. Thus, the two components of HD 434 are rotating 6–8 times more rapidly than their pseudosynchronous values.

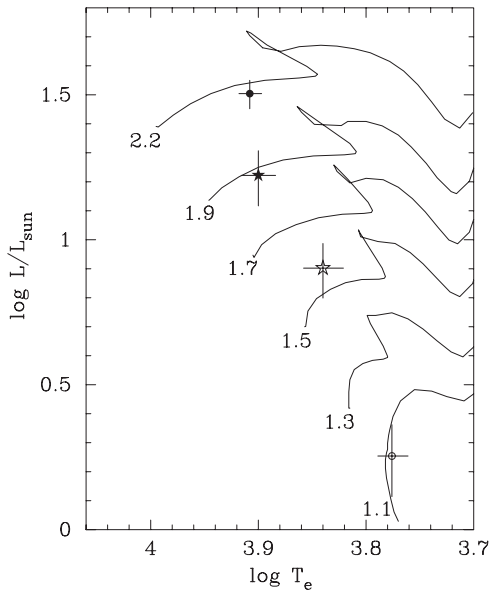


Figure 5. Positions of the components of HD 434 (stars) and 41 Sex (circles) are compared with the 1.1, 1.3, 1.5, 1.7, 1.9, and $2.2 M_{\odot}$ solar-abundance evolutionary tracks of Girardi et al. (2000) in a theoretical H-R diagram. The more massive component in each system corresponds to the filled symbol. Our estimated uncertainties are shown.

7.2. 41 Sex

To determine whether the components of 41 Sex are synchronously rotating, we compute equatorial velocities from our projected rotational velocities and then compare them with the predicted pseudosynchronous velocities. For 41 Sex our $v \sin i$ values, averaged from 35 spectra for the primary and 29 spectra for the secondary, are 20 ± 1 and 7 ± 3 km s⁻¹, respectively. Fekel (2003) obtained a $v \sin i$ value of 21 km s⁻¹ from a small subset of our spectra. The minimum masses of the two components (Table 5) are relatively small compared to the expected masses for their spectral types (Gray 1992). Thus, we compare the position of the primary in the H-R diagram with the solar abundance evolutionary tracks of Girardi et al. (2000), which produces a mass estimate of $2.18 M_{\odot}$. That value, combined with the $m \sin^3 i$ value of the primary, results in an orbital inclination of 54° , which by chance is the same value that we have estimated for HD 434. If the axes of the rotational and orbital inclinations are parallel, then the observed equatorial rotational velocities are 25 and 9 km s⁻¹. The synchronous rotational velocities for the primary and secondary, computed with our radii from the Stefan–Boltzmann law, are 24 and 10 km s⁻¹, respectively. Thus, we conclude that both the primary and secondary are rotating synchronously. This result accords with theory, since the binary orbit is already circularized.

8. LINE DEPTHS OF 41 SEX

From 66 and 33 Å mm⁻¹ photographic spectra, Sreedhar Rao et al. (1990) presented evidence that the primary of 41 Sex has phase-modulated line depth variations. They stated that many blended metallic lines in their blue wavelength spectra have depth changes of 10%–20% and appear to systematically peak in strength around orbital phases 0.25, 0.50, 0.75, and 1.0, relative to the time of maximum positive velocity. They argued that these line depth changes were similar to those seen in various metal lines of Ap stars and so likely had a similar explanation. The hallmark of this latter class of peculiar stars

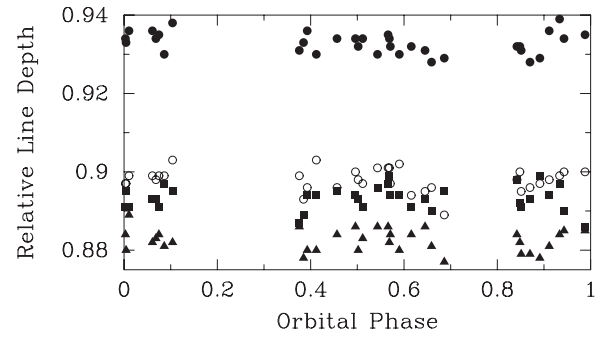


Figure 6. Relative line depths vs. orbital phase for four lines of the 41 Sex primary. Zero phase is a time of maximum positive velocity. Solid circles: Fe I at 6393.612 Å, open circles: Fe I at 6400.009 Å, squares: Fe II at 6416.928 Å, and triangles: Ca I at 6439.083 Å.

Table 6
Line Depths of 41 Sex

Ion	Wavelength (Å)	Mean Line Depth	Sigma
Fe I	6393.612	0.933	0.003
Fe I	6400.009	0.898	0.003
Fe II	6416.928	0.893	0.003
Ca I	6439.083	0.883	0.003

is that they have much stronger than normal absorption lines of rare earth elements (Lueftinger et al. 2003), produced by very strong magnetic fields that have caused those particular elements to coalesce into localized surface regions. As an Ap star rotates, periodic changes in the strength of these lines are seen. The technique of Doppler imaging provides surface maps of the changing distributions (e.g., Lueftinger et al. 2003).

As a result of their analysis, Sreedhar Rao et al. (1990) concluded that the Am star primary of 41 Sex has characteristics that link the Am and Ap groups. However, they did caution that higher resolution CCD spectra would be useful to confirm the spectral line variations. Worek’s ongoing interest in the 41 Sex system led him to obtain such observations. His careful analysis of new blue wavelength spectra (Worek 1998) did *not* confirm the results of Sreedhar Rao et al. (1990), and he suggested alternative possible reasons for the line variability claimed by Sreedhar Rao et al. (1990).

We analyzed 34 red wavelength KPNO spectra to examine further the possible line depth changes in the primary of 41 Sex. Our spectra typically have signal-to-noise ratios of 200–300. Although the red region of the spectrum is far less crowded than the blue region, the metal lines are generally much weaker than those at blue wavelengths. Table 6 lists the two Fe I lines, one Fe II line, and one Ca I line that we measured. The spectra were normalized to unity and the continuum rectified. A Gaussian curve was fitted to each observed line profile. The depths (one minus the residual intensity) of the four lines are plotted versus the orbital phase in Figure 6, and the average depth and standard deviation are listed in Table 6. The orbital phases are those given in Table 4, where the zero phase is a time of maximum velocity of the primary. Despite gaps in our phase coverage near orbital conjunctions at phases 0.25 and 0.75, we find no line variations at the relative intensity level of 0.01–0.02 suggested by the results of Sreedhar Rao et al. (1990). The depths of all four lines have $\sigma = 0.003$ (Table 6), and for three of the four lines, 82% of the line depths are within 1σ of the average values. The exception is the Fe II line, which has 74% of its measures within

1σ . Like Worek (1998), we are unable to confirm the results of Sreedhar Rao et al. (1990).

9. CONCLUSIONS

We have detected the secondary component in two previously known spectroscopic binaries, HD 434 and 41 Sex, and for the first time determined double-lined orbits for them. Because the secondary lines of HD 434 were previously unresolved, several of our orbital elements are substantially different from earlier solutions. With the detection of the faint secondary component of 41 Sex we have enhanced the utility of that system for the determination of its basic properties.

We have confirmed the conclusion of Iliev et al. (2001) that both components of HD 434 are Am stars. The primary of 41 Sex is also an Am star, while its secondary component is a late-F or early-G dwarf. Comparison with evolutionary tracks indicates that all four stars are still on the main sequence.

The components of HD 434 are rotating 6–8 times faster than their predicted pseudosynchronous velocities. On the other hand, the components of 41 Sex are rotating synchronously.

From the *Hipparcos* parallaxes and adopted masses of the two systems we have estimated the maximum angular separations of the components. The orbit of HD 434 is eccentric, and so we determined its maximum nodal separation (e.g., McAlister 1976; Halbwegs 1981) of 3.3 mas. The orbit of 41 Sex is circular, enabling us, like Halbwegs (1981), to use Kepler's third law to estimate an angular semimajor axis of 1.0 mas. Although these separations are small, they are within the scope of modern optical interferometers. Thus, when our spectroscopic results are complemented with high-quality interferometric results, accurate three-dimensional orbits, masses, and distances for the systems will follow.

For the primary in 41 Sex we measured the line depths of four metal lines. Like Worek (1998), we are unable to confirm the 10%–20% line depth variations claimed by Sreedhar Rao et al. (1990).

We thank J. Tomkin for providing us with his velocities from the 2.1 m telescope at McDonald Observatory. The help of Daryl Willmarth in support of the KPNO coude feed observations is appreciated. The research at Tennessee State University was supported in part by NASA grant NCC5-511 and NSF grant HRD-9706268.

REFERENCES

- Abt, H. A. 1961, *ApJS*, **6**, 37
 Abt, H. A. 2004, *ApJS*, **155**, 175
 Abt, H. A., & Levy, S. G. 1985, *ApJS*, **59**, 229
 Abt, H. A., & Morrell, N. I. 1995, *ApJS*, **99**, 135
 Barden, S. C. 1985, *ApJ*, **295**, 162
 Barker, E. S., Evans, D. S., & Laing, J. D. 1967, *R. Obs. Bull.*, **130**, 355
 Batten, A. H., Fletcher, J. M., & MacCarthy, D. G. 1989, *Publ. Dom. Astrophys. Obs.*, **17**, 1
 Bertaud, Ch. 1970, *A&AS*, **1**, 7
 Boden, A. F., Torres, G., & Latham, D. W. 2006, *ApJ*, **644**, 1193
 Budaj, J., Iliev, I. Kh., Barzova, I. S., Ziznovsky, J., Zverko, J., & Stateva, I. 2003, *IBVS*, **5423**, 1
 Cowley, A., Cowley, C., Jaschek, M., & Jaschek, C. 1969, *AJ*, **74**, 375
 Cunha, M. S. 2007, *A&AR*, **14**, 217
 Eaton, J. A., & Williamson, M. H. 2004, *Proc. SPIE*, **5496**, 710
 Eaton, J. A., & Williamson, M. H. 2007, *PASP*, **119**, 886
 Fekel, F. C. 1997, *PASP*, **109**, 514
 Fekel, F. C. 2003, *PASP*, **115**, 807
 Fekel, F. C., Boden, A. F., Tomkin, J., & Torres, G. 2009a, *ApJ*, **695**, 1527
 Fekel, F. C., Tomkin, J., & Williamson, M. H. 2009b, *AJ*, **137**, 3900
 Fekel, F. C., Tomkin, J., & Williamson, M. H. 2010, *AJ*, **139**, 1579
 Flower, P. J. 1996, *ApJ*, **469**, 355
 Girardi, L., Bressan, A., Bertelli, G., & Chiosi, C. 2000, *A&AS*, **141**, 371
 Gray, D. F. 1992, *The Observation and Analysis of Stellar Photospheres* (Cambridge: Cambridge Univ. Press)
 Halbwegs, J. L. 1981, *A&AS*, **44**, 47
 Hoffleit, D. 1982, *The Bright Star Catalogue* (4th rev. ed.; New Haven, CT: Yale Univ. Observatory)
 Hube, D. P., & Gulliver, A. F. 1985, *J. R. Astron. Soc. Canada*, **79**, 49
 Huenemoerder, D. P., & Barden, S. C. 1984, *BAAS*, **16**, 510
 Hummel, C. A., et al. 2001, *AJ*, **121**, 1623
 Hut, P. 1981, *A&A*, **99**, 126
 Iliev, I. Kh., Budaj, J., Ziznovsky, J., & Zverko, J. 2001, *IBVS*, **5051**, 1
 Johnson, H. L. 1966, *ARA&A*, **4**, 193
 Lucy, L. B., & Sweeney, M. A. 1971, *AJ*, **76**, 544
 Lueftinger, T., Kuschnig, R., Piskunov, N. E., & Weiss, W. W. 2003, *A&A*, **406**, 1033
 Margoni, R., Munari, U., & Stagni, R. 1992, *A&AS*, **93**, 545
 Matthews, L. D., & Mathieu, R. D. 1992, in *ASP Conf. Ser.* 32, *Complimentary Approaches to Double and Multiple Star Research*, IAU Colloq. 135, ed. H. A. McAlister & W. I. Hartkopf (San Francisco, CA: ASP), 244
 McAlister, H. A. 1976, *PASP*, **88**, 317
 McCarthy, J. A., Sandiford, B. A., Boyd, D., & Booth, J. 1993, *PASP*, **105**, 881
 Palmer, D. R., Walker, E. N., Jones, D. H. P., & Wallis, R. E. 1968, *R. Greenwich Obs. Bull.*, **135**, 385
 Perryman, M. A. C., et al. 1997, *A&A*, **323**, L49
 Pourbaix, D., et al. 2004, *A&A*, **424**, 727
 Quirrenbach, A. 2001, *ARA&A*, **39**, 353
 Royer, F., Grenier, S., Baylac, M.-O., Gomez, A. E., & Zorec, J. 2002, *A&A*, **393**, 897
 Scarfe, C. D., Batten, A. H., & Fletcher, J. M. 1990, *Publ. Dom. Astrophys. Obs.*, **18**, 21
 Shajn, G. A. 1951, *Izv. Krymsk Astrofiz. Obs.*, **7**, 124
 Sreedhar Rao, S., & Abhyankar, K. D. 1992, *MNRAS*, **258**, 819
 Sreedhar Rao, S., Abhyankar, K. D., & Nagar, P. 1990, *ApJ*, **365**, 336
 Stockton, R. A., & Fekel, F. C. 1990, *MNRAS*, **256**, 575
 Strassmeier, K. G., & Fekel, F. C. 1990, *A&A*, **230**, 389
 Tassoul, J.-L., & Tassoul, M. 1992, *ApJ*, **395**, 259
 Tomkin, J., & Fekel, F. C. 2006, *AJ*, **131**, 2652
 Tomkin, J., & Fekel, F. C. 2008, *AJ*, **135**, 555
 Torres, G., Andersen, J., & Giménez, A. 2010, *A&AR*, **18**, 67
 van Leeuwen, F. 2007, *A&A*, **474**, 653
 Walker, N. 1966, *Observatory*, **86**, 154
 Wolfe, R. H., Horak, H. G., & Storer, N. W. 1967, in *Modern Astrophysics*, ed. M. Hack (New York: Gordon & Breach), 251
 Worek, T. F. 1998, *PASP*, **110**, 580
 Worek, T. F., Beardsley, W. R., & King, M. W. 1978, *AJ*, **83**, 303
 Worek, T. F., Zizka, R., King, M. W., & Beardsley, W. R. 1986, *PASP*, **98**, 238
 Zahn, J.-P. 1977, *A&A*, **57**, 383